

Scroll Waves and Filaments in excitable Media of higher spatial Dimension

Marie Cloet^{1,2}, Louise Arno^{1,2}, Desmond Kabus^{1,2,3}, Joeri Van der Veken⁴, Alexander V. Panfilov^{5,6,7}, and Hans Dierckx^{1,2*}

¹Department of Mathematics, KU Leuven Campus Kortrijk (KULAK), Kortrijk, Belgium, ²iSi Health, Institute of Physics-based Modeling for In Silico Health, KU Leuven, Leuven, Belgium, ³Laboratory of Experimental Cardiology, Leiden University Medical Center (LUMC), Leiden, The Netherlands,

⁴Department of Mathematics, KU Leuven, Leuven, Belgium,

⁵Department of Physics and Astronomy, Ghent University, Ghent, Belgium,

⁶Laboratory of Computational Biology and Medicine, Ural Federal University, Ekaterinburg, Russia,

⁷World-Class Research Center “Digital biodesign and personalized healthcare”, Sechenov University, Moscow, Russia

(Dated: May 1, 2023)

Excitable media are ubiquitous in nature, and in such systems the local excitation tends to self-organize in traveling waves, or in rotating spiral-shaped patterns in two or three spatial dimensions. Examples include waves during a pandemic or electrical scroll waves in the heart. Here we show that such phenomena can be extended to a space of four or more dimensions and propose that connections of excitable elements in a network setting can be regarded as additional spatial dimensions. Numerical simulations are performed in four dimensions using the FitzHugh-Nagumo model, showing that the vortices rotate around a two-dimensional surface which we define as the superfilament. Evolution equations are derived for general superfilaments of co-dimension two in an N -dimensional space and their equilibrium configurations are proven to be minimal surfaces. We suggest that biological excitable systems, such as the heart or brain which have non-local connections can be regarded, at least partially, as multidimensional excitable media and discuss further possible studies in this direction.

Introduction. Many real-world systems exhibit a large non-linear response to external or internal stimuli, and are therefore called excitable systems. In the continuum limit, several of these systems are reasonably understood, as unifying geometric principles have been revealed that enable us to understand and quantify their dynamics. As a first example, non-linear traveling waves of constant amplitude have been observed as depolarization waves in neural [1] and cardiac tissue [2], combustion [3] or oxidation [4] processes, Mexican waves in crowds [5], and infection waves in a pandemic [6]. This extremely diverse range of phenomena has been described mathematically in the continuum limit using reaction-diffusion equations

$$\partial_t \mathbf{u} = \mathbf{P} \Delta_N \mathbf{u} + \mathbf{F}(\mathbf{u}), \quad (1)$$

where $\mathbf{u}(\vec{r}, t)$ is a state vector with S components that varies in N -dimensional space and time, and \mathbf{P} is a diagonal $S \times S$ matrix containing the diffusivity of each state variable, Δ_N the Laplacian operator in N spatial dimensions and $\mathbf{F}(\mathbf{u})$ a local excitation model. The state vector can support waves and it was shown mathematically that their wave fronts undergo curvature-driven dynamics, with the lowest order effect behaving like surface tension [7–9]. These curvature effects are governed by the medium characteristics, mathematically represented by the model parameters. Wave fronts are known to be lines in two-dimensional (2D) media, and surfaces in 3D media. This property can be summarized as wave

fronts having spatial co-dimension $C = 1$, i.e., they are $(N - C)$ -dimensional structures in an N -D space.

In observations of excitable surfaces ($N = 2$), excitation patterns were often found to organize into rotating spiral-shaped patterns. Their study is largely motivated by cardiological applications, since electrical rotors have been observed on the surface of the heart during rhythm disorders. Like for wave fronts, spiral waves drift is affected by geometric factors, such as the local Gaussian curvature of the excitable surface [10], possibly incorporating anisotropy of wave propagation within the surface [11]. Spiral waves on a surface rotate around a core region, which is commonly idealized into a phase singularity (PS) point, of co-dimension 2 [12]. The case where quasi-periodically moving (meandering) PSs occur is more involved, and has been described recently [13–15]. In 3D media, such as cardiac tissue, a stack of spiral waves is known as a scroll wave. A scroll wave rotates around a curve consisting of PSs, the filament which has codimension $N - C = 3 - 2 = 1$. The curvature-induced dynamics of filaments was first established numerically in [16–18] for isotropic excitable media where they were shown to exhibit so-called filament tension [19], a medium-dependent emerging parameter. For positive filament tension, filaments straighten up [17, 18], while for negative filament tension, filaments elongate and tend to break up [16], if the medium is thick enough [20]. In the context of cardiac arrhythmias, the topological configuration of filament curves in the cardiac wall (e.g., O, I or U-shaped) is being used as a classifier for arrhythmia patterns. Moreover, spatio-temporal drift (due to internal interaction or gradients in the medium) is thought to be responsible for transitions between arrhythmias [21].

* h.dierckx@kuleuven.be

From the above overview on the current knowledge, a natural question arises that is at first sight purely mathematical: Which other patterns of co-dimension C exist in N -dimensional media? In this paper, we provide some answers to these questions. We confirm that indeed other patterns exist, more specifically, superfilaments ($C = 2$), i.e., the organizing center of superscrolls in a space with $N = 4$ spatial dimensions.

Research hypothesis. We claim that such higher dimensional patterns are significant for real-world excitable systems. The crucial point is that simulations on an N -D grid are related to a regular network of connected excitable elements. Indeed, when the aforementioned systems in $N = 2$ or $N = 3$ spatial dimensions are studied numerically, they are often simulated on a Cartesian grid with lattice constant h . Using the second order accurate Laplacian stencil (see Fig. 1), the discretization of Eq. (1) for the i -th node in the grid becomes

$$\partial_t \mathbf{u}_i = \mathbf{P} \sum_{j:A_{ij}=1} \frac{\mathbf{u}_j - \mathbf{u}_i}{h^2} + \mathbf{F}(\mathbf{u}_i). \quad (2)$$

Here, $A_{ij} = 1$ if the node i is next to j and 0 otherwise. In \mathbb{R}^1 , every interior point will have 2 such neighbors, in \mathbb{R}^2 , 4 neighbors, etc. Thus, if one will discretize similarly the Laplacian in \mathbb{R}^4 , every interior point will have 8 neighbors and in \mathbb{R}^N , one obtains $2N$ such neighbors. Note, however, that Eq. (2) can also be regarded as an excitable network [22], where A_{ij} is the adjacency matrix of the graph consisting of the edges that form the network. In this view, going to $N > 3$ actually makes sense, as an idealized model for excitable networks in which each node is connected to $2N$ neighbors. In network language, such graph would be a limit of a translationally invariant network with average degree $2N$, also called a regular network. In view of real-world networks with unexplained emergent pattern formation, N can grow large. For example, on social networks, the average degree is of magnitude $10^2 - 10^3$ [23]. In brain tissue, cerebellar granule cells make about 675 synaptic connections with Purkinje cells, which in their turn receive input from around 185,000 parallel fibers [24]. If a networks with high degree is realized in 3D space that surrounds us, it implies that the network exhibits long-range, or global connections. Within this work, we will consider in simulations only one extra dimension, such that $N = 4$, which already shows interesting new physical phenomena. Analytical results below are obtained for any integer $N > 2$.

Methods. Traveling wave solutions have been realized before in the radially symmetric case for $N = 4$, see [9]. To demonstrate the existence of scroll waves in $N = 4$, we initiate a classical scroll wave ($C = 2$) rotating in the XY-plane. The filament then has dimension $N - C = 2$ and hence will be a surface, which we call the superfilament.

To this purpose, the reaction-diffusion system (1) was integrated numerically using the Euler method, with an N -dimensional hypercube as the domain: $\vec{r} \in [0, L]^N$. In each dimension, space was discretized uniformly, resulting in a lattice with spacing h . Values of h are

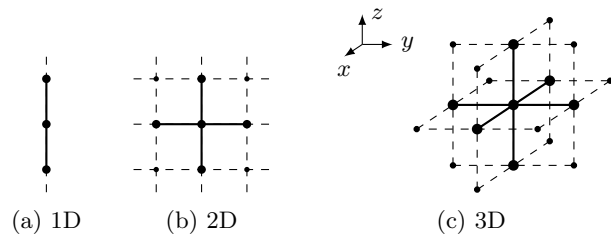


Figure 1: Stencil for the second order accurate discretization of the Laplacian in 1D, 2D and 3D. Nodes connected to the central point obtain a weight $1/h^2$, see Eq. (2).

mentioned with each simulation results and were chosen small enough such that no discretization artifacts could be observed in the state variable fields. For the local excitation dynamics $\mathbf{F}(\mathbf{u})$, we chose the FitzHugh-Nagumo (FHN) kinetics with parameters according to the excitable (non-oscillatory) regime [25]: $\mathbf{u} = [u, v]^T$, $\mathbf{F} = [f(u, v), g(u, v)]^T$ with

$$f = \epsilon^{-1} \left(u + \frac{u^3}{3} - v \right), \quad g = \epsilon(u - av + b) \quad (3)$$

and $\mathbf{P} = \text{diag}(1, 0)$, meaning that only u is diffused. The constants ϵ , a and b are parameters determining the model dynamics. In this paper, they are chosen in the excitable regime. The FHN was originally formulated for neural conduction, but has been applied equally to continuous models of cardiac excitation [26]. As such, it is well suited to explore the boundary between discrete and continuous excitation models.

To initiate the scroll in N dimensions, we first applied classical cross-field stimulation. Let us denote the 4 spatial coordinate axes as X, Y, Z and A . To start a scroll rotating in a plane, e.g., the XY-plane, we use the S1-S2 protocol, with translational symmetry in the two dimensions perpendicular to this plane.

To visualize the superfilament surface, we looped over all points of the medium at given sampling times, to see if any of them lied at the intersection of the hypersurfaces $u = 0$ and $v = 0$. Hereto, the algorithm of Fenton and Karma [27] was applied in every coordinate plane.

Numerical results. By using a spherical S1 and a rectangular S2, a first curved superfilament is created, see Fig. 2a. In intersections parallel to the XY-plane, a spiral wave is observed, while in the other 5 coordinate planes, traveling waves are seen. The curved filament was seen to flatten over time, similar to wave fronts with positive surface tension [7] and filaments with positive tension [19].

Secondly, we created a hole in the superfilament by selecting a cylindrical region at the center of the medium, perpendicular to the superfilament, and set the medium to the resting state there. Remarkably, the rim of the superfilament does not stay in the same plane, but moves at some angle to it, reminiscent of the pseudoscalar filament tension component of classical scrolls [19].

In a third simulation, we created a superfilament in 4D that is anchored to 2 obstacles at opposite domain boundaries, to test the minimal principle for classical rotor filaments by Wellner *et al.* [28]. The result in Fig. 2c suggests that indeed a minimal principle holds, and that the equilibrium configuration will be a minimal surface. This conjecture will be proven below.

In summary, our numerical simulations show that superscrolls and superfilaments exist in 4D and that their motion is tightly linked to geometric factors.

Analytical results. Motivated by the numerical results of Fig. 2, the equation of motion for the superfilaments of co-dimension $C = 2$ will be derived here, inspired by previous results in 2 and 3 dimensions [8, 19, 29]. In those works, a scroll wave was constructed by stacking a set of spiral waves along a filament curve. In an N -dimensional domain, the superfilament \mathcal{F} will be a $(N - 2)$ -dimensional submanifold that can be parameterized as $x^i = X^i(\sigma^m)$, with coordinates σ^m , where $m = 1, 2, \dots, N - 2$ and $i = 1, 2, \dots, N$. In one point of \mathcal{F} , we construct 2 orthogonal unit normal vectors \vec{N}_A , with $A \in \{1, 2\}$. The spatial change of these vectors between different points on the submanifold is given by the Weingarten formula [30]:

$$D_m \vec{N}_A = -S_{\vec{N}_A}(\vec{e}_m) + \nabla_m^\perp \vec{N}_A. \quad (4)$$

Here, D_m is the derivative in \mathbb{R}^N in the direction of coordinate σ^m , $S_{\vec{N}_A}$ is the shape operator inherited from the normal direction \vec{N}_A and \vec{e}_m is the tangent vector to \mathcal{F} corresponding to coordinate direction σ^m . The second term $\nabla_m^\perp \vec{N}_A$ is the normal connection, describing the relative rotation of both normals when one moves along the superfilament. This term can be set to 0 by choosing the normal vectors \vec{N}_1 and \vec{N}_2 to be parallel with respect to the normal connection. This procedure is similar to constructing a relative parallel frame to a curve in 3D [31]. The first term in Eq. (4) describes the local curvature of the filament, in terms of the shape operator.

Next, we introduce normal coordinates ρ^A for points in the vicinity of the superfilament:

$$x^i = X^i(\sigma^m) + \sum_{A=1}^2 \rho^A N_A^i. \quad (5)$$

This allows us to define the normal vectors \vec{N}_A also in the vicinity of the superfilament, by $N_A^i = \frac{\partial x^i}{\partial \rho^A}$. The divergence of \vec{N}_A is then related to the curvature of the superfilament. Indeed, by construction, $D_B \vec{N}_A = 0$ for $A, B \in \{1, 2\}$, such that with Eq. (4) we obtain [30, 32]:

$$\text{div}(\vec{N}_A) = \sum_{m=1}^{N-2} \vec{e}_m \cdot D_m \vec{N}_A = -\text{tr}(S_{\vec{N}_A}) = -\vec{N}_A \cdot \vec{H}, \quad (6)$$

with \vec{H} the (non-normalized) mean curvature of the superfilament.

With these preparations, we can now explicitly construct the superscroll as a stack of spiral wave solutions. Say $\mathbf{U}(x, y; \phi)$ is a spiral wave solution in the 2D plane, rotated around the origin over an angle ϕ . Then, we propose as a solution to Eq. (1) in N dimensions:

$$\begin{aligned} \mathbf{u}(x^i, t) &= \mathbf{U}(\rho^1, \rho^2, \phi(\sigma^m, t)) + \tilde{\mathbf{u}}(x^i, t), \\ \phi(\sigma^m, t) &= \omega + \tilde{\omega}(\sigma^m, t) \end{aligned} \quad (7)$$

where ω is the spiral's natural rotation frequency in a plane. This approximation is a gradient expansion around a planar superfilament, and the $\tilde{\mathbf{u}}$ and $\tilde{\omega}$ are higher-order corrections in the extrinsic curvature of the superfilament, similar to earlier work on classical scroll wave filaments [8, 29]. Substituting the expressions in the RDE brings, after reordering terms,

$$\dot{\mathbf{u}} - \hat{\mathbf{L}}\tilde{\mathbf{u}} = \sum_{A=1}^2 \left[\mathbf{P} \text{div}(\vec{N}_A) + (\vec{N}_A \cdot \dot{\vec{X}}) \right] \frac{\partial \mathbf{U}}{\partial \rho^A} + \omega \frac{\partial \mathbf{U}}{\partial \phi}, \quad (8)$$

where $\hat{\mathbf{L}} = \mathbf{P}\Delta_2 + \omega\partial_\phi + \mathbf{F}'(\mathbf{U})$. This operator only depends on the standard 2D unperturbed rotating spiral solution. From symmetry arguments, it is known to have critical eigenmodes (Goldstone modes), as well as spatially localized adjoint eigenfunctions [8, 29, 33–36], also known as response functions [35]. Taking the overlap integral of Eq. (8) with the response functions delivers, after averaging over one rotation period [19, 29]:

$$\dot{\vec{X}} = -\gamma_1 \sum_{A=1}^2 \text{div}(\vec{N}_A) \vec{N}_A - \gamma_2 \sum_{A,B=1}^2 \varepsilon_{AB} \text{div}(\vec{N}_B) \vec{N}_A, \quad (9)$$

Here, γ_1 and γ_2 are the scalar and pseudoscalar filament tension coefficients that were introduced in [19] and ε_{AB} are the components of the Levi-Civita symbol $\vec{\varepsilon} = \begin{pmatrix} 0 & 1 \\ -1 & 0 \end{pmatrix}$. Using Eq. (6) we can express the superfilament dynamics in terms of its mean curvature:

$$\dot{\vec{X}} = \gamma_1 \vec{H} + \gamma_2 \vec{\varepsilon} \cdot \vec{H}, \quad (10)$$

Our result is consistent with the lower-dimensional case: for $N = 3$, the superfilament becomes a filament curve with arc length s , curvature k , tangent vector \vec{T} and unit normal \vec{N} , then $\vec{H} = k\vec{N} = \frac{\partial \vec{T}}{\partial s}$. Then, Eq. (10) reduces to the classical result of Biktashev *et al.* [19].

From the equation of motion (10), it follows that stationary superfilaments must have $\vec{H} = \vec{0}$, thus the total mean curvature must vanish. For the case $N = 4$, this means that a stationary superfilament must be a minimal surface, generalizing Wellner's minimal principle to superscrolls [28]. It proves a property that we postulated before based on an action principle [37], see also Fig. 2c.

Similar to wave fronts and classical filaments, the motion of superfilaments in a homogeneous medium is driven by curvature. It is possible to explicitly show that in the case of positive filament tension, the superfilament will decrease its size, as follows. From the variational

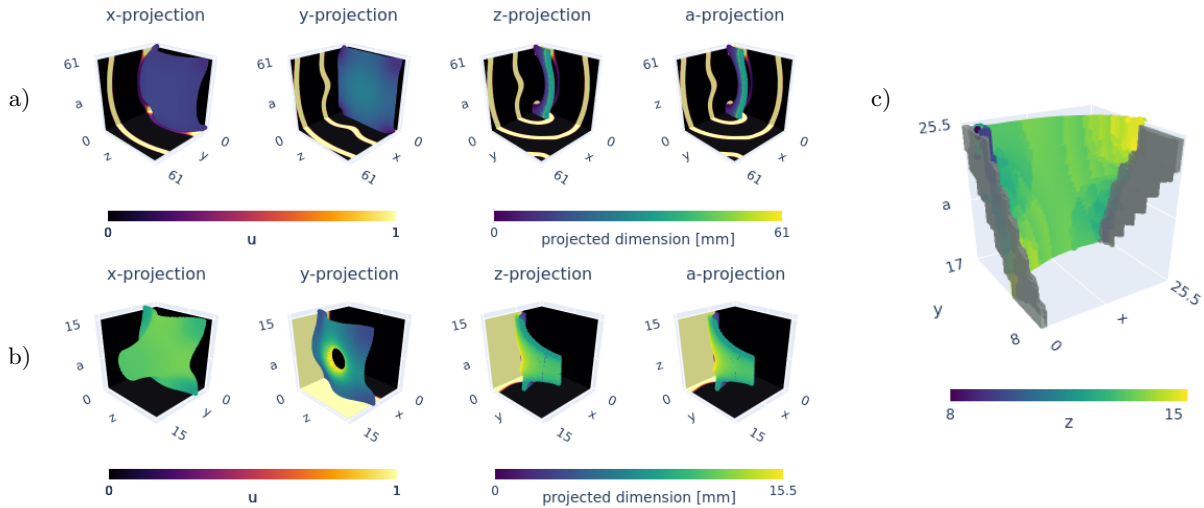


Figure 2: Superscrolls rotating around superfilaments in a 4D reaction-diffusion system (Eq. (1)). Exactly n grid points of spacing h were used in each dimension. (a) A superscroll rotating around a 2D curved superfilament ($n = 61, h = 1$ mm). Four visualizations of the same timeframe are shown, each time with a different dimension rendered as color of the superfilament. The bottom of the medium is colored according to local excitation intensity u . (b) A pierced superfilament ($n = 31, h = 0.5$ mm), shown using 4 projects as in (a). (c) A superfilament anchored to non-parallel obstacles (shaded in grey) at opposite domain boundaries ($n = 51, h = 0.5$ mm).

derivative of the surface area [38, 39], $\frac{\delta S}{\delta X^i} = -H^i$, it follows that

$$\begin{aligned} \frac{dS}{dt} &= \int_{\mathcal{F}} \frac{\delta S}{\delta X^j} \frac{\partial X^j}{\partial t} dV \\ &= - \int_{\mathcal{F}} \vec{H} \cdot [\gamma_1 \vec{H} + \gamma_2 \vec{\varepsilon} \cdot \vec{H}] dV = -\gamma_1 \int_{\mathcal{F}} \|\vec{H}\|^2 dV \end{aligned} \quad (11)$$

with dV the volume form and $\|\cdot\|$ the Euclidean norm of a vector. Eq. (11) gives the analogue of the change-of-length rate $dL/dt = -\gamma_1 \int k^2 ds$ for classical filaments [19], which we retrieve as the case $N = 3$. We have here shown that superfilaments monotonically decrease their length in case of positive filament tension. As a corollary, stable superscrolls can persist in excitable media as minimal surfaces (or their higher-dimensional counterparts), e.g., by anchoring to opposite boundaries of the medium, as in [28, 37]. In principle, also stable knotted structures may exist [40], but this investigation falls outside our present scope. Conversely, if $\gamma_1 < 0$, classical filaments are known to destabilize, which is named as a possible pathway from ventricular tachycardia in the heart to fibrillation [20, 41]. Based on Eqs. (10),(11), this phenomenon can also occur in higher-dimensional media.

The numerical results of Fig. 2a-c can now be better understood in light of our geometric theory. Parameter values were chosen to correspond to $\gamma_1 > 0$ for a scroll wave in 3D. All panels show flattening over time of the superfilament. In panel (b), the shrinking of the hole in the filament does not occur in the plane of the superfilament, but according to Eq. (10) at an angle to it, since $\gamma_2 \neq 0$ for this system, reminiscent of the oblique drift of classi-

cal filaments under an external perturbation [19, 42].

Discussion. We have shown via simulations that adding a fourth spatial dimension to a reaction-diffusion systems yields new structures: a superscroll and a superfilament. Moreover, we have formalized the superfilament dynamics by means of a geometric derivation. It is expected that even more complex structures will arise when the number of dimensions N , or the co-dimension C of the structure is further increased.

Our motivation for this research is the link between Laplacian stencils used for simulations according to the Euler method (see Fig. 1) and regular networks [22]. Having demonstrated the phenomenology of the predicted and simulated structures, we can here deepen the discussion and potential. When the classical scroll waves and filament were introduced in cardiology, for example, they enabled a better understanding of the emergent patterns seen at the outer surface of the heart. Also, the distance-weighted averaging of the excitation patterns is reflected in the electrical recordings near the heart or on the body surface, and the properties of the scroll wave are now known to affect the frequencies present in the electrograms [43].

With this Letter, we aim to open up research on scrolls in more dimensions, here called superscrolls, in relation to non-linear excitation dynamics in networks. Several additional facts will have to be accounted for. First, we assume here a regular, translationally invariant network. In realistic networks, this condition is typically not met. However, locally there will be closed loops along which the excitation dynamics can travel and re-excite; we leave open the possibility that its description may re-

quire also a non-integer number of dimensions [44]. Secondly, the properties of a network typically vary between the excitable elements. Heterogeneity of excitable nodes can be dealt with as a gradient as in cardiac modeling, whereas the local variations in nodal degree (i.e., number of connections) may require a probabilistic approach to describe the dynamics of excitation structures such as wavefronts and (super)scrolls. Thirdly, in our derivation of curvature-driven dynamics, a linear coupling between elements was assumed: Eq. (2) describes a flow proportional to the difference in state variables at either side of an edge. Such effective coupling is also traditional in cardiac tissue modeling, although it is known that signal conduction consists of a traveling wave along the cell membrane interleaved with conduction over gap junctions to the next cell.

Finally, we suggest to search in general for superscrolls in real-life systems, as they may offer geometric insight in yet unknown mechanisms. In this search, the notion of excitability can be taken very broadly, as any arrangement of elements that can respond to stimuli with a non-linear response. Examples in human society may include spreading of opinions or epidemics. In technology, contamination, combustions, (temporary) failure and overflow may provide examples. Also oscillatory media may host superscrolls, but there the distinction with phase waves needs to be made.

Conclusion. In this work, we introduced a mathematical generalization of scroll waves and filaments to N -dimensional Euclidean space. Superfilaments were shown to obey curvature-driven dynamics and an area-minimizing principle in case of positive tension. Al-

though the world around us is only three-dimensional (omitting possible compactified dimensions), we conjecture that superscrolls can occur in media where oscillatory or excitable elements are connected on average to more than $2N$ neighbors, i.e., in networks with non-local connections, such as neural tissues, and social, biochemical or technological networks.

ACKNOWLEDGMENTS

A. V. Panfilov is grateful to A.S. Mikhailov for helpful discussions. M. Cloet was funded by KU Leuven grant STG/19/007 L. Arno was funded by a FWO-Flanders fellowship, grant 117702N. D. Kabus is supported by KU Leuven grant GPUL/20/012. H. Dierckx and computational infrastructure were funded by KU Leuven grant STG/19/007. J. Van der Veken is supported by the Research Foundation Flanders (FWO) and the National Natural Science Foundation of China (NSFC) under collaboration project G0F2319N, by the KU Leuven Research Fund under project 3E210539 and by the Research Foundation Flanders (FWO) and the Fonds de la Recherche Scientifique (FNRS) under EOS Projects G0H4518N and G0I2222N. A. V. Panfilov's research at Sechenov University was financed by the Ministry of Science and Higher Education of the Russian Federation within the framework of state support for the creation and development of World-Class Research Centers Digital biodesign and personalized healthcare (Grant No 075-15-2022-304).

-
- [1] P. C. Bressloff, *Waves in Neural Media: From Single Neurons to Neural Fields*, Lecture Notes on Mathematical Modelling in the Life Sciences (Springer, New York, NY, 2014).
 - [2] R. Clayton, O. Bernus, E. Cherry, H. Dierckx, F. Fenton, L. Mirabella, A. Panfilov, F. Sachse, G. Seemann, and H. Zhang, *Progress in Biophysics and Molecular Biology* **104**, 22 (2011).
 - [3] Y. Zeldovich and D. Frank-Kamenetsky, *Acta. Physicochim.* **274**, 341 (1938).
 - [4] A. B. Rovinskii and A. M. Zhabotinskii, *The Journal of Physical Chemistry* **88**, 6081 (1984), publisher: American Chemical Society.
 - [5] I. Farkas, D. Helbing, and T. Vicsek, *Nature* **419**, 131 (2002), number: 6903 Publisher: Nature Publishing Group.
 - [6] J. Medlock and M. Kot, *Mathematical Biosciences* **184**, 201 (2003).
 - [7] S. Koga and Y. Kuramoto, *Progress of Theoretical Physics* **63**, 106 (1980).
 - [8] J. P. Keener, *Physica D: Nonlinear Phenomena* **31**, 269 (1988).
 - [9] H. Dierckx, O. Bernus, and H. Vershelde, *Physical Review Letters* **107**, 108101 (2011).
 - [10] A. Mikhailov, V. Davydov, and V. Zykov, *Physica D: Nonlinear Phenomena* **70**, 1 (1994).
 - [11] H. Dierckx, E. Brisard, H. Vershelde, and A. V. Panfilov, *Physical Review E* **88**, 012908 (2013).
 - [12] R. A. Gray, A. M. Pertsov, and J. Jalife, *Nature* **392**, 75 (1998).
 - [13] N. Tomii, M. Yamazaki, T. Ashihara, K. Nakazawa, N. Shibata, H. Honjo, and I. Sakuma, *Computers in Biology and Medicine* **130**, 104217 (2021).
 - [14] L. Arno, J. Quan, N. Nguyen, M. Vanmarcke, T. E.M., and H. Dierckx, *Front. Physiol.* **12** (2021), 10.3389/fphys.2021.690453.
 - [15] D. Kabus, L. Arno, L. Leenknecht, A. V. Panfilov, and H. Dierckx, *PloS One* **17**, e0271351 (2022).
 - [16] A. Panfilov and A. Rudenko, *Physica D: Nonlinear Phenomena* **28**, 215 (1987).
 - [17] A. Panfilov and A. Pertsov, *Doklady AN SSSR* **274**, 1500 (1984).
 - [18] A. Panfilov, A. Rudenko, and V. Krinsky, *Biofizika* **31**, 850 (1987).
 - [19] V. N. Biktashev, *Philosophical Transactions of the Royal Society of London. Series A: Physical and Engineering Sciences* **347**, 611 (1994).
 - [20] H. Dierckx, H. Vershelde, S. Selsil, and V. N. Biktashev, *Physical Review Letters* **109**, 174102 (2012).
 - [21] J. Jalife, R. A. Gray, G. E. Morley, and J. M. Davidenko,

- Chaos: An Interdisciplinary Journal of Nonlinear Science **8**, 79 (1998), publisher: American Institute of Physics.
- [22] H. Nakao and A. S. Mikhailov, *Nature Physics* **6**, 544 (2010).
- [23] S. A. Myers, A. Sharma, P. Gupta, and J. Lin, in *Proceedings of the 23rd International Conference on World Wide Web, WWW '14 Companion* (Association for Computing Machinery, New York, NY, USA, 2014) pp. 493–498.
- [24] R. J. Harvey and R. M. A. Napper, *Progress in Neurobiology* **36**, 437 (1991).
- [25] R. FitzHugh, *Biophysical Journal* **1**, 445 (1961).
- [26] I. V. Biktasheva, A. V. Holden, and V. N. Biktashev, *International Journal of Bifurcation and Chaos* **16**, 1547 (2006).
- [27] F. Fenton and A. Karma, *Chaos: An Interdisciplinary Journal of Nonlinear Science* **8**, 20 (1998).
- [28] M. Wellner, O. Berenfeld, J. Jalife, and A. M. Pertsov, *Proceedings of the National Academy of Sciences* **99**, 8015 (2002).
- [29] H. Vershelde, H. Dierckx, and O. Bernus, *Physical Review Letters* **99**, 168104 (2007).
- [30] J. M. Lee, *Introduction to Riemannian Manifolds*, Graduate Texts in Mathematics, Vol. 176 (Springer International Publishing, Cham, 2018).
- [31] R. Bishop, *Am. Math. Mon.* **82**, 264 (1975).
- [32] M. Dajczer and R. Tojeiro, *Submanifold Theory: Beyond an Introduction*, Universitext (Springer US, New York, NY, 2019).
- [33] D. Barkley, *Physical Review Letters* **72**, 164 (1994), publisher: American Physical Society.
- [34] H. Henry and V. Hakim, *Physical Review E* **65**, 046235 (2002).
- [35] I. V. Biktasheva and V. N. Biktashev, *Physical Review E* **67**, 026221 (2003).
- [36] I. V. Biktasheva, D. Barkley, V. N. Biktashev, G. V. Bordyugov, and A. J. Foulkes, *Physical Review E, Statistical, Nonlinear, and Soft Matter Physics* **79**, 056702 (2009).
- [37] H. Dierckx, M. Wellner, O. Bernus, and H. Vershelde, *Physical Review Letters* **114**, 178104 (2015).
- [38] H. Dierckx and H. Vershelde, *Physical Review E* **93**, 022210 (2016), publisher: American Physical Society.
- [39] C. Baker, *The Mean Curvature Flow of Submanifolds of High Codimension*, Ph.D. thesis, Australian National University (2010).
- [40] J. P. Keener and J. J. Tyson, *SIAM Review* **34**, 1 (1992).
- [41] A. V. Panfilov, *Chaos: An Interdisciplinary Journal of Nonlinear Science* **8**, 57 (1998), publisher: American Institute of Physics.
- [42] H. Dierckx, O. Bernus, and H. Vershelde, *Phys D* **238**, 941 (2009).
- [43] Z. Qu and A. Garfinkel, in *Cardiac Electrophysiology (Fourth Edition)*, edited by D. P. Zipes and J. Jalife (W.B. Saunders, 2004) pp. 327–335.
- [44] T. Wen and K. H. Cheong, *Information Fusion* **73**, 87 (2021).